Electromagnetically induced transparency with superradiant and subradiant states

Wei Feng, Da-Wei Wang, Han Cai, Shi-Yao Zhu, and Marlan O. Scully

Phys. Rev. A **95**, 033845 — Published 31 March 2017

DOI: 10.1103/PhysRevA.95.033845

Electromagnetically Induced Transparency with Superradiant and Subradiant states

Wei Feng,[1,2] Da-Wei Wang,[2,*] Han Cai,[2] Shi-Yao Zhu,[1,3] and Marlan O. Scully[2,4,5]

[1] *Beijing Computational Science Research Center, Beijing 100193, China*
[2] *Texas A&M University, College Station, TX 77843, USA*
[3] *Department of Physics, Zhejiang University, Hangzhou 310027, China*
[4] *Baylor University, Waco, Texas 76706, USA*
[5] *Xi'an Jiaotong University, Xi'an, Shaanxi 710048, China*

We construct the electromagnetically induced transparency (EIT) by dynamically coupling a superradiant state with a subradiant state. The superradiant and subradiant states with enhanced and inhibited decay rates act as the excited and metastable states in EIT, respectively. Their energy difference determined by the distance between the atoms can be measured by the EIT spectra, which renders this method useful in subwavelength metrology. The scheme can also be applied to many atoms in nuclear quantum optics, where the transparency point due to counter-rotating wave terms can be observed.

PACS numbers: 42.50.Nn, 42.50.Ct

I. INTRODUCTION

Electromagnetically induced transparency (EIT) [1, 2] is a quantum optical mechanism that is responsible for important phenomena such as slow light [3–5], quantum memory [6–8] and enhanced nonlinearity [9, 10]. A probe field that resonantly couples the transition from the ground state $|g\rangle$ to an excited state $|e\rangle$ of an atom, experiences a transparency point at the original Lorentzian absorption peak, if the excited state is coherently and resonantly coupled to a metastable state $|m\rangle$. EIT involves at least three levels and naturally three-level atoms are used in most cases. However, proper three-level structures are not available in some optical systems, such as in atomic nuclei [11–13] and biological fluorescent molecules [14], in which EIT can have important applications once realized. Interestingly, it has been shown that even with only two-level systems, EIT-like spectra can be achieved by locally addressing the atomic ensembles [15–17]. However, strict EIT scheme with a dynamic coupling field is still absent in two-level optical systems.

Superradiance and subradiance are the enhanced and inhibited collective radiation of many atoms [18–20], associated with the collective Lamb shifts [21–23]. The superradiance and subradiance of two interacting atoms has attracted much interest both theoretically [24, 25] and experimentally [26–30]. In this paper, we use superradiance and subradiance to construct EIT and investigate the new feature in the EIT absorption spectrum involving with the cooperative effect and the counter-rotating wave terms. For only two atoms, the symmetric (superradiant) state has much larger decay rate than the anti-symmetric (subradiant) state when the distance between the two atoms is much smaller than the transition wavelength. These two states serve as the excited and the metastable states and their splitting, depending on the distance between the atoms, can be measured by the EIT spectra. In addition, the counter-rotating wave terms in the effective coupling field between the superradiant and subradiant states bring an additional transparency point, which is usually not achievable in traditional EIT systems with three-level atoms.

This paper is organized as following. In Sec. II, we introduce the basic mechanism with two atoms and show its application in subwavelength metrology. In Sec. III, we extend the mechanism to many atoms and show the additional EIT point due to the counter-rotating terms. Finally, we make conclusion in Sec. IV. The detailed calculations are put into the Appendices.

II. MECHANISM

Two two-level atoms have four quantum states, a ground state $|gg\rangle$, two first excited states $|ge\rangle$ and $|eg\rangle$, and a double excited state $|ee\rangle$. Considering the interaction between the two atoms, the eigen basis of the first excited states is composed by the symmetric and anti-symmetric states (independent of the distance and the dipole interaction between the two atoms [23]),

$$\begin{aligned} |+\rangle &= \frac{1}{\sqrt{2}}\left[|eg\rangle + |ge\rangle\right], \\ |-\rangle &= \frac{1}{\sqrt{2}}\left[|eg\rangle - |ge\rangle\right], \end{aligned} \tag{1}$$

with decay rates $\gamma_\pm = \gamma_0 \pm \gamma_c$ and energy shifts $\Delta_\pm = \pm\Delta_c$. Here γ_0 is the single atom decay rate, γ_c and Δ_c are the collective decay rate and energy shift (see Appendix A). When the distance between the two atoms $r \ll \lambda$ where λ is the transition wavelength, we have $\gamma_c \to \gamma_0$ and thus $\gamma_+ \to 2\gamma_0$ and $\gamma_- \to 0$. The collective energy shift Δ_c is divergent with $1/r^3$. A weak probe field can only resonantly excite $|+\rangle$ from $|gg\rangle$ since the collective energy shift Δ_c moves the transition between $|+\rangle$ and $|ee\rangle$ out of resonant with the probe field [29]. We can

* whatarewe@tamu.edu

neglect the two-photon absorption for a weak probe field [28, 31]. The states $|gg\rangle$, $|+\rangle$ and $|-\rangle$ form a three-level system, as shown in Fig. 1 (a). The symmetric and the anti-symmetric states satisfy the requirement on the decoherence rates for EIT, i.e., $\gamma_+ \gg \gamma_-$ when $r \ll \lambda$. The eigenenergies of $|\pm\rangle$ states are split by the collective energy shift.

The challenge is how to resonantly couple $|+\rangle$ and $|-\rangle$ states. The key result of this paper is that $|+\rangle$ and $|-\rangle$ states can be coupled by two off-resonant counter-propagating plane waves with different frequencies ν_1 and ν_2. If the frequency difference $\nu = \nu_1 - \nu_2$ matches the splitting between $|+\rangle$ and $|-\rangle$ states $2\Delta_c$, we obtain on resonance coupling via two Raman transitions as shown in Fig. 1 (b). The resulting Hamiltonian is (assuming $\hbar = 1$) (see Appendix B),

$$\begin{aligned} H =& \omega_+|+\rangle\langle+| + \omega_-|-\rangle\langle-| + \Omega_c(t)(|+\rangle\langle-| + |-\rangle\langle+|) \\ & - \Omega_p(e^{-i\nu_p t}|+\rangle\langle gg| + h.c.), \end{aligned} \tag{2}$$

where $\Omega_c(t) = \Omega_0 \sin(kr)\sin(\nu t - \phi)$ with $k = \nu_s/c$, $\nu_s = (\nu_1+\nu_2)/2$, $r = x_1 - x_2$ and $\phi = k(x_1+x_2)$ with $x_{1,2}$ being the coordinates of the two atoms along the propagation of the plane waves. The coupling strength $\Omega_0 = E^2d^2/(\omega - \nu_s)$ with E being the amplitude of the electric field of the plane waves, d being the transition matrix element of the atoms and ω being the single atom transition frequency. The transition frequencies of $|\pm\rangle$ states are $\omega_\pm = \omega \pm \Delta_c + \delta_u(t)$ with $\delta_u(t) = \Omega_0[1 + \cos(kr)\cos(\nu t - \phi)]$ being a universal Stark shift induced by the two plane waves.

The absorption spectra can be calculated by the Liouville equation,

$$\begin{aligned} \frac{\partial \rho}{\partial t} =& -i[H, \rho] + \sum_{j=+,-} \frac{\gamma_j}{2}[2|gg\rangle\langle j|\rho|j\rangle\langle gg| \\ & - |j\rangle\langle j|\rho - \rho|j\rangle\langle j|]. \end{aligned} \tag{3}$$

Since H is time-dependent with frequency ν, the coherence can be expanded $\langle+|\rho|gg\rangle = \sum_n \rho^{[n]}_{+gg} e^{in\nu t}$. Eq.(3) can be solved with the Floquet theorem [32, 33] and the absorption is proportional to $\mathrm{Im}\rho^{[0]}_{+gg}$, the imaginary part of the zero frequency coherence (see Appendix C).

The counter-rotating wave terms of $\Omega_c(t)$ can be neglected for small distance between the two atoms and weak coupling field when $\Omega_0 \sin(kr) \ll \Delta_c$. We obtain typical EIT absorption spectra with two absorption peaks and one transparency point, as shown in the black curve of Fig. 2 (a). Here the probe detuning $\delta_p = \omega + \Delta_c + \Omega_0 - \nu_p$ has taken into account all the static energy shifts of $|+\rangle$ state, including Ω_0, the static part of the universal Stark shift $\delta_u(t)$. The effect of the counter-rotating wave terms and the universal shift $\delta_u(t)$ emerge either when we increase the distance (reduce Δ_c) between the two atoms or increase the dynamic Stark shift Ω_0 (proportional to the intensity of the standing wave), which are demonstrated by the multiple side peaks in Fig. 2 (a).

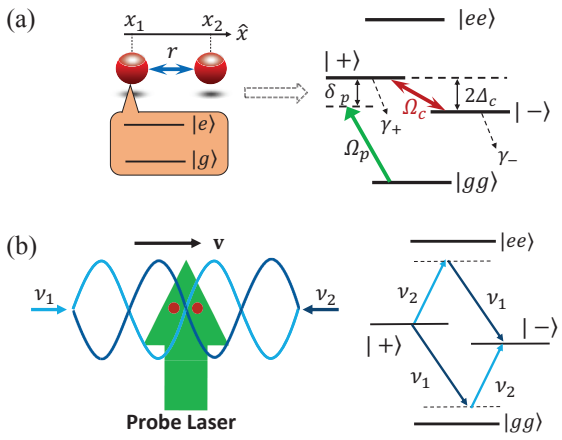

FIG. 1. (Color online) (a) Two two-level atoms form an EIT system with the symmetric (superradiant) state being the excited state and the anti-symmetric (subradiant) state being the metastable state. (b) The symmetric and anti-symmetric states are resonantly coupled by the Raman transitions of two counter-propagating plane waves. We can also understand this coupling as induced by the time-dependent difference between the dynamic Stark shifts of the two atoms induced by a moving standing wave with velocity $\mathbf{v} = \nu\hat{x}/2k$.

We can use the following procedure for the subwavelength metrology, as shown in Fig. 2 (b). We first reduce the intensity of the standing wave to only allow two peaks to appear in the spectra. Then we tune the frequency difference ν until the two absorption peaks become symmetric, which yields the collective energy shift $\Delta_c = \nu/2$. The distance between the two atoms can be obtained by the relation between $\Delta_c(r)$ and r (see Appendix A). Since $\Delta_c(r) \propto 1/r^3$ for small distance $r \ll \lambda$, the sensitivity $\delta\Delta_c/\delta r \propto 1/r^4$. Compared with the existing proposals for subwavelength imaging of two interacting atoms with fluorescences [34], a natural preference for this EIT metrology is that both the dressing field and the probe fields are weak. This is in particular useful for the biological samples that cannot sustain strong laser fields. This scheme which depends on the interaction between two atoms is different from the Heisenberg limit metrology based on superradiance with timed Dicke states, where the momentum of photons are stored in non-interacting atomic ensembles [35].

The above mechanism can also be understood as a dynamic modulation of the transition frequency difference between the two atoms (see Appendix B). We notice that the difference between $|+\rangle$ and $|-\rangle$ states is a relative π phase factor between $|eg\rangle$ and $|ge\rangle$ states. If we can control the transition frequencies of the two atoms such that the states $|eg\rangle$ and $|ge\rangle$ have energy shifts Ω_c and $-\Omega_c$ respectively, an initial state of the symmetric state $|\psi(0)\rangle = |+\rangle$ evolves with time $|\psi(t)\rangle = (e^{-i\Omega_c t}|eg\rangle + e^{i\Omega_c t}|ge\rangle)/\sqrt{2}$. At $t = \pi/2\Omega_c$, we obtain

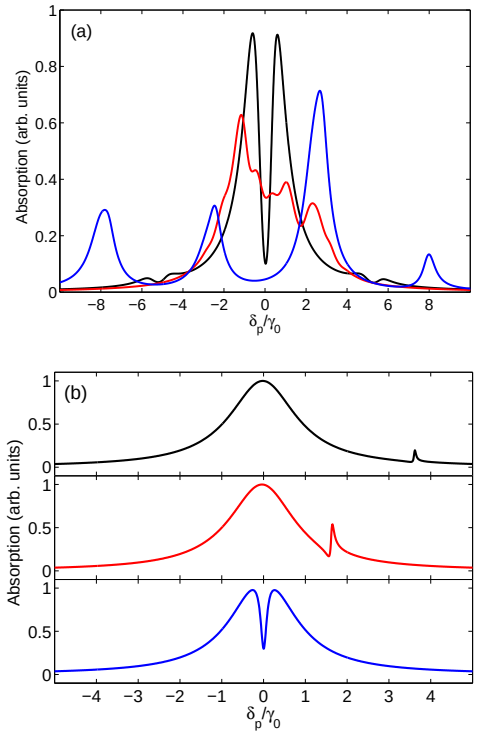

FIG. 2. (Color online) Absorption spectra of two-atom superradiance EIT. (a) The absorption spectra for different distances r and Rabi frequencies Ω_0. Black line: $r = 0.1\lambda$ ($\Delta_c = 2.60\gamma_0$, $\gamma_c = 0.92\gamma_0$), $\Omega_0 = 2\gamma_0$; red line: $r = 0.2\lambda$ ($\Delta_c = 0.38\gamma_0$, $\gamma_c = 0.71\gamma_0$), $\Omega_0 = 2\gamma_0$ and blue line: $r = 0.1\lambda$, $\Omega_0 = 10\gamma_0$. The coupling field is on resonance for each case, $\nu = 2\Delta_c$. (b) The absorption spectra with different standing wave detunings. $\nu = 7\gamma_0$ (black line) $9\gamma_0$ (red line) $10.5\gamma_0$ (blue line). $\Omega_0 = \gamma_0$. When $\nu = 10.5\gamma_0 = 2\Delta_c$, the absorption spectrum is symmetric. From the relation between Δ_c and r, we obtain the distance between the two atoms $r = 0.08\lambda_0$, which agrees with the parameters that we set.

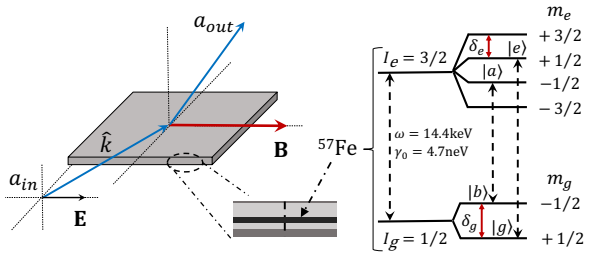

FIG. 3. Superradiance EIT in nuclear quantum optics. A thin-film cavity is probed by hard x-rays with grazing angle incidence. The ^{57}Fe nuclei are embedded in the center of the cavity. We add an oscillating magnetic field parallel to the electric field of the linearly polarized incident x-ray. Only the two transitions denoted by the dashed arrows between the magnetic Zeeman levels can happen. The energy difference of these two transitions serve as the effective coupling between the superradiant and subradiant states. The EIT spectra can be detected with the reflected signal.

$|\psi(t)\rangle = -i|-\rangle$. Therefore, the states $|+\rangle$ and $|-\rangle$ are coupled by an energy difference between the two atoms. In our scheme, the two counter propagating plane waves create a moving standing wave that induces a time-dependent dynamic Stark shift difference between the two atoms, $\Omega_c(t)$, which serves as the coupling field. This picture enables us to generalize the mechanism to many atoms, as shown later.

The single atom EIT [36] and the superradiance and subradiance of two ions [27] have been observed in experiments. The coupling between the symmetric and anti-symmetric states has also been realized with two atoms trapped in an optical lattice [37]. In particular, the cryogenic fluorescence of two interacting terrylene molecules has been used for spectroscopy with nanometer resolution [28]. Due to different local electric fields, the two molecules have different transition frequencies, which corresponds to a static coupling field Ω_c. By introducing an oscillating electric field gradient or a moving standing wave, such a system can be exploited for the current EIT experiment of superradiance and subradiance. Very recently, superradiance was also observed from two silicon-vacancy centers embedded in diamond photonic crystal cavities [38], which provide another platform to realize this mechanism.

Once the EIT is achieved, we can realize other related phenomena. In particular, we can use the adiabatic population transfer to prepare the subradiant state $|-\rangle$, which has a long life time for quantum memory [8]. This can be done by adiabatically tuning down Ω_0 and tuning up Ω_p at the two-photon resonance. The maximum value of Ω_p should be smaller than Δ_c to avoid populating the $|ee\rangle$ state.

III. GENERALIZATION TO MANY ATOMS

The mechanism can be extended to large ensembles of two-level systems. Let us consider two atomic ensembles, one with $|e\rangle$ and $|g\rangle$, and the other with $|a\rangle$ and $|b\rangle$ as their excited and ground states. Each ensemble has N atoms and both ensembles are spatially mixed together. The transition frequency difference between the two atomic ensembles is within the linewidth such that a single photon can excite the two ensembles to a superposition of two timed Dicke states [39, 40],

$$|+_{\mathbf{k}}\rangle = \frac{1}{\sqrt{2}}(|e_{\mathbf{k}}\rangle + |a_{\mathbf{k}}\rangle) \tag{4}$$

where

$$|e_{\mathbf{k}}\rangle = \frac{1}{\sqrt{N}}\sum_{n=1}^{N} e^{i\mathbf{k}\cdot\mathbf{r}_n}|g_1, ..., e_n, ..., g_N\rangle \otimes |b_1, b_2, ..., b_N\rangle,$$

$$|a_{\mathbf{k}}\rangle = |g_1, g_2, ..., g_N\rangle \otimes \frac{1}{\sqrt{N}}\sum_{n=1}^{N} e^{i\mathbf{k}\cdot\mathbf{s}_n}|b_1, ..., a_n, ..., b_N\rangle. \tag{5}$$

Here $\mathbf{r}_n$ and $\mathbf{s}_n$ are the positions of the nth atom in the two ensembles. $\mathbf{k}$ is the wave vector of the single photon. The timed Dicke states $|e_\mathbf{k}\rangle$ and $|a_\mathbf{k}\rangle$ are excited from the same ground state $|G\rangle \equiv |g_1, g_2, ..., g_N\rangle \otimes |b_1, b_2, ..., b_N\rangle$ by a single photon. They have directional emission in the direction of $\mathbf{k}$, so as their superposition state $|+_\mathbf{k}\rangle$, associated with enhanced decay rate and collective Lamb shift. On the other hand, the state

$$|-_\mathbf{k}\rangle = \frac{1}{\sqrt{2}}(|e_\mathbf{k}\rangle - |a_\mathbf{k}\rangle), \tag{6}$$

is a subradiant state in the sense that its decay rate is estimated to be similar to that of a single atom [41]. The directional emissions of $|e_\mathbf{k}\rangle$ and $|a_\mathbf{k}\rangle$ are canceled because of the relative phase factor -1 between them. The collective Lamb shift of $|-_\mathbf{k}\rangle$ can be very different from that of the $|+_\mathbf{k}\rangle$ state.

We can dynamically couple $|+_\mathbf{k}\rangle$ and $|-_\mathbf{k}\rangle$ states in a well studied nuclear quantum optical system [11, 40, 42], as shown in Fig. 3. The nuclei embedded in a waveguide are ^{57}Fe with the transition frequency $\omega = 14.4$keV and the linewidth $\gamma_0 = 4.7$neV. In the presence of a magnetic field, the ground and excited states with $\mathrm{I}_g = 1/2$ and $\mathrm{I}_e = 3/2$ split into multiplets with Zeeman energy splitting δ_j $(j = e, g)$. Applying a magnetic field $\mathbf{B}$ parallel to the incident and outgoing electric fields $\mathbf{E}_{\rm in}$ and $\mathbf{E}_{\rm out}$ and perpendicular to $\mathbf{k}$, the linearly polarized input x-ray can only couple two transitions, as shown in Fig. 3. At room temperature, the populations on the two magnetic sublevels of the ground state are approximately equal [40]. Here we can use a magnetically soft ^{57}FeNi absorber foil with zero magnetostriction [13] to avoid the mechanical sidebands and other complications in a time-dependent external magnetic field.

The Hamiltonian in the interaction picture can be written as,

$$\begin{aligned} H =& \Omega_c(t)(|+_\mathbf{k}\rangle\langle -_\mathbf{k}| e^{-i\omega_0 t} + |-_\mathbf{k}\rangle\langle +_\mathbf{k}| e^{i\omega_0 t}) \\ & - \Omega_p(e^{-i\delta_p t}|+_\mathbf{k}\rangle\langle G| + h.c.), \end{aligned} \tag{7}$$

where $\Omega_c(t) = \Omega_1 \cos(\nu t)$ with $\Omega_1 = (\delta_g + \delta_e)/2$ is induced by a magnetic field $B = B_0 \cos \nu t$. ω_0 is the collective Lamb shift difference between the states $|+_\mathbf{k}\rangle$ and $|-_\mathbf{k}\rangle$. δ_p is the probe detuning from the $|+_\mathbf{k}\rangle$ state. The reflectance of the thin film cavity is dominated by the coherence $|\rho_{+G}|^2$ where $\rho_{+G} \equiv \langle +_\mathbf{k}|\rho|G\rangle$ (see Appendix D),

$$|R|^2 \propto \lim_{T\to\infty} \frac{1}{T} \int_0^T |\rho_{+G}(t)|^2 \mathrm{d}t = \sum_n \left|\rho_{+G}^{[n]}\right|^2, \tag{8}$$

where we have made average in a time interval $T \gg 1/\nu$. The coherence ρ_{+G} has multiple frequency components $\rho_{+G}(t) = \sum_n \rho_{+G}^{[n]} e^{i2\nu t}$ due to the counter-rotating wave terms. Only when $\nu = 0$, no time average is needed.

The typical collective Lamb shift of ^{57}Fe nuclear ensemble is $5 \sim 10\gamma_0$ [11]. The internal magnetic field in the ^{57}Fe sample can be tens of Tesla in an external radio-frequency field [13, 43]. The effective coupling field Rabi frequency Ω_1 can be easily tuned from zero to $20\gamma_0$. The magnetic field amplitudes corresponding to the effective coupling strengths $\Omega_1 = 5\gamma_0$ and $\Omega_1 = 20\gamma_0$ taken in Fig. 4 (a) and (b) are $B_0 = 5.3$T and $B_0 = 21.3$T, respectively.

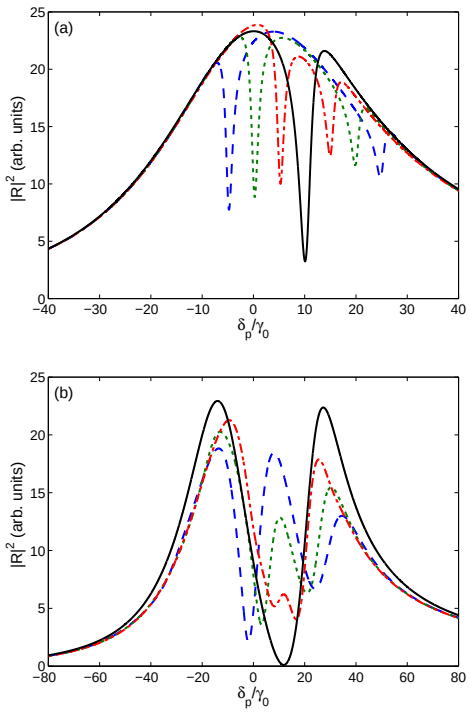

FIG. 4. (Color online) The reflectance of x-ray with effective Rabi frequencies (a) $\Omega_1 = 5\gamma_0$ and (b) $\Omega_1 = 20\gamma_0$. The decay rates of $|+_\mathbf{k}\rangle$ and $|-_\mathbf{k}\rangle$ are $\gamma_+ = 50\gamma_0$ and $\gamma_- = \gamma_0$. The collective Lamb shift difference $\omega_0 = 10\gamma_0$. The oscillation frequencies of the magnetic fields are $\nu = 15\gamma_0$ (blue dash line), $10\gamma_0$ (green dot line), $5\gamma_0$ (red dash dot line) and 0 (black solid line).

The reflectance spectra can be used to investigate the effect of the counter-rotating wave terms of the coupling field and to determine the collective Lamb shift. For a relatively small Ω_1, there are two dips in a single Lorentzian peak, as shown in Fig. 4 (a). The left and right ones correspond to the rotating and counter-rotating wave terms of the coupling field, respectively. The distance between the two dips is approximately 2ν. When $\nu = 0$, these two dips merge and the spectrum is the same as the one of the previous EIT experiments with a static coupling between two ensembles mediated by a cavity [15]. For a larger $\Omega_1 = 20\gamma_0$ in Fig. 4 (b), we still have the two dips since $\Omega_1 < \gamma_+$ and the vacuum induced coherence still exists [42], but we also have two peaks basically corresponding to the two magnetic transitions in Fig. 3. Compared with the result in [40] where $|+_\mathbf{k}\rangle$ and $|-_\mathbf{k}\rangle$ have the same energy and the magnetic field is static, here the two peaks are not symmetric for $\nu = 0$ due to a

finite Lamb shift difference. Therefore, the results can be compared with experimental data to obtain the collective Lamb shifts.

IV. CONCLUSION

We construct an EIT scheme by dynamically coupling the superradiant state with the subradiant state. The interaction between atoms can be measured by the EIT spectra. Compared with the EIT-like schemes with a static coupling in atomic ensembles [15, 17, 40, 42, 44], the local dynamical modulation of the transition frequencies of the atoms introduces a tunable detuning for the coupling field. Therefore, our scheme contains all the ingredients of EIT. In particular, for the systems where the splitting between the superradiant and subradiant states is larger than the decay rate of the superradiant state, the dynamic modulation can bring the EIT dip to the Lorentzian absorption peak of the superradiant state, as shown in Fig. 2 (b). The dynamic modulation enables a precise measurement of the distance between two atoms and brings new physics of the EIT point due to counter-rotating wave terms.

The authors thank G. Agarwal, A. Akimov, A. Belyanin, J. Evers, W. Ge, O. Kocharovskaya, W.-T. Liao, Z. Liao, R. Röhlsberger and A. Sokolov for insightful discussions. We acknowledge the support of National Science Foundation Grant EEC-0540832 (MIRTHE ERC), Office of Naval Research (Award No. N00014-16-1-3054) and Robert A. Welch Foundation (Grant No. A-1261). Wei Feng was supported by China Scholarship Council (Grant No. 201504890006). H. Cai is supported by the Herman F. Heep and Minnie Belle Heep Texas A&M University Endowed Fund held/administered by the Texas A&M Foundation.

APPENDIX A. COLLECTIVE DECAY RATE AND ENERGY SHIFT

In the bare basis of two two-level atoms, the master equation for the density matrix is ($\hbar = 1$) [20]

$$\begin{aligned}\frac{\partial\rho}{\partial t} =& -i[H,\rho] - i\Delta_c \sum_{i\neq j=1}^{2}[\sigma_i^+\sigma_j^-,\rho] \\ &- \sum_{i,j=1}^{2}\frac{\gamma_{ij}}{2}(\sigma_i^+\sigma_j^-\rho - 2\sigma_j^-\rho\sigma_i^+ + \rho\sigma_i^+\sigma_j^-),\end{aligned} \tag{9}$$

where $\sigma_i^+ \equiv |e_i\rangle\langle g_i|$ and $\sigma_i^+ \equiv |g_i\rangle\langle e_i|$ are the raising and lowering operators of the ith atom. Here $\gamma_{11} = \gamma_{22} = \gamma_0$ is the single atom radiative decay rate, $\gamma_0 = d^2\omega^3/(3\pi\varepsilon_0 c^3)$ where d is the dipole moment, ω is the transition frequency, ε_0 is the vacuum permittivity and c is the speed of light in vacuum. $\gamma_{12} = \gamma_{21} = \gamma_c$ and Δ_c are the collective decay rate and collective energy shift,

$$\begin{aligned}\gamma_c =& \frac{3}{2}\gamma_0\left\{\sin^2\eta\frac{\sin k_0 r}{k_0 r}\right. \\ &\left. + \left(1-3\cos^2\eta\right)\left[\frac{\cos k_0 r}{(k_0 r)^2} - \frac{\sin k_0 r}{(k_0 r)^3}\right]\right\},\end{aligned} \tag{10}$$

$$\begin{aligned}\Delta_c =& \frac{3}{4}\gamma_0\left\{-\sin^2\eta\frac{\cos k_0 r}{k_0 r}\right. \\ &\left. + \left(1-3\cos^2\eta\right)\left[\frac{\sin k_0 r}{(k_0 r)^2} + \frac{\cos k_0 r}{(k_0 r)^3}\right]\right\},\end{aligned} \tag{11}$$

where η is the angle between the dipole moment $\mathbf{d}$ and the two-atom displacement $\mathbf{r}$, $k_0 = \omega/c$ is the magnitude of the transition wave vector.

All through this paper, we adopt $\eta = \pi/2$, which means that the transition dipole moment and also the probe light polarization is perpendicular to the line connecting the two atoms. This assumption, of course, is just for the sake of simplicity. We can change η by exciting different transition dipoles with probe light polarized in the corresponding directions.

APPENDIX B. EFFECTIVE COUPLING BETWEEN SYMMETRIC AND ANTI-SYMMETRIC STATES

The result of the effective coupling $\Omega_c(t)$ can be obtained by calculating the second order transition strength between $|+\rangle$ and $|-\rangle$ states via the moving standing wave, as shown in Fig. 1 (b). The interaction Hamiltonian of two counter-propagating plane waves coupled with the two atoms is

$$\begin{aligned}H_d =& \frac{Ed}{2}e^{-i\nu_1 t}(e^{ikx_1}\sigma_1^+ + e^{ikx_2}\sigma_2^+) \\ &+ \frac{Ed}{2}e^{-i\nu_2 t}(e^{-ikx_1}\sigma_1^+ + e^{-ikx_2}\sigma_2^+) + h.c..\end{aligned} \tag{12}$$

In the following, we calculate the Raman transition matrix elements between $|+\rangle$ and $|-\rangle$ states in the effective Hamiltonian. Starting from $|+\rangle$ state, the atoms can emit a ν_1 photon and transit to $|gg\rangle$ state and then absorb a ν_2 photon to transit to $|-\rangle$ state. The matrix element is

$$\begin{aligned}&\frac{E^2d^2}{4(\omega-\nu_1)}|-\rangle\langle -|e^{-i\nu_2 t}(e^{-ikx_1}\sigma_1^+ + e^{-ikx_2}\sigma_2^+)|gg\rangle \\ &\langle gg|e^{i\nu_1 t}(e^{-ikx_1}\sigma_1^- + e^{-ikx_2}\sigma_2^-)|+\rangle\langle +| \\ =&\frac{E^2d^2}{8(\omega-\nu_1)}e^{i\nu t}(e^{-2ikx_1} - e^{-2ikx_2})|-\rangle\langle +|.\end{aligned} \tag{13}$$

The atoms can also first absorb a ν_2 photon and transit to $|ee\rangle$ state, and then emit a ν_1 photon and transit to

$|-\rangle$ state, The matrix element is

$$\begin{aligned}&-\frac{E^2d^2}{4(\omega-\nu_2)}|-\rangle\langle-|e^{i\nu_1 t}(e^{-ikx_1}\sigma_1^- + e^{-ikx_2}\sigma_2^-)|ee\rangle\\ &\langle ee|e^{-i\nu_2 t}(e^{-ikx_1}\sigma_1^+ + e^{-ikx_2}\sigma_2^+)|+\rangle\langle+|\\ =&\frac{E^2d^2}{8(\omega-\nu_2)}e^{i\nu t}(e^{-2ikx_1} - e^{-2ikx_2})|-\rangle\langle+|.\end{aligned} \tag{14}$$

Under the condition in our paper, we can take $\omega-\nu_1 = \omega-\nu_2 = \omega-\nu_s$. The total matrix element between $|+\rangle$ and $|-\rangle$ states is the summation of Eqs. (13) and (14),

$$\frac{E^2d^2}{\omega-\nu_s}\frac{e^{i\nu t-i\phi}}{2i}\sin(kr)|-\rangle\langle+|, \tag{15}$$

which is the rotating-wave coupling between $|+\rangle$ and $|-\rangle$ states. All other terms in $\Omega_c(t)$ and the universal energy shifts $\delta_u(t)$ can be calculated in a similar way.

Alternatively, we can also obtain the effective interaction Hamiltonian by calculating the dynamic Stark shifts of the two atoms. The two atoms are dressed by a moving standing wave $E_s = E\cos(\nu_1 t - k_1 x) + E\cos(\nu_2 t + k_2 x)$ with detuning between forward and backward fields $\nu \equiv \nu_1 - \nu_2$. Under the condition that $\nu \ll \nu_1, \nu_2$, the standing wave can be rewritten as

$$E_s = 2E\cos(\nu_s t)\cos(\nu t/2 - kx), \tag{16}$$

where $\nu_s = (\nu_1+\nu_2)/2$ and $k = (k_1+k_2)/2$. Under the rotating-wave approximation (RWA) and in a rotating frame, the single atom time-dependent Hamiltonian can be written as

$$H_s(t) = \begin{bmatrix} \omega-\nu_s & Ed\cos(\nu t/2-kx) \\ Ed\cos(\nu t/2-kx) & 0 \end{bmatrix}, \tag{17}$$

The time-dependent eigenvalues of the Hamiltonian are

$$\begin{aligned}E_\pm(t) =&\frac{1}{2}(\omega-\nu_s)\\ &\pm\frac{1}{2}\sqrt{(\omega-\nu_s)^2 + 4E^2d^2\cos^2(\nu t/2-kx)}.\end{aligned} \tag{18}$$

In the limit that $Ed \ll |\omega-\nu|$, the dynamic shift of the transition frequency is

$$\Delta_S = E_+ - E_- - (\omega-\nu_s) = \frac{2E^2d^2\cos^2(\nu t/2-kx)}{\omega-\nu_s}. \tag{19}$$

Since the two atoms have two different positions at x_1 and x_2, they have different dynamic Stark shift. We rewrite the dressed Hamiltonian of the two atoms in the basis of symmetric and anti-symmetric states:

$$\begin{aligned}H_d(t) =&\Delta_S(x_1)|eg\rangle\langle eg| + \Delta_S(x_2)|ge\rangle\langle ge|\\ =&\Omega_c(t)(|+\rangle\langle-| + |-\rangle\langle+|) + \delta_u(t)(|+\rangle\langle+|\\ &+|-\rangle\langle-|),\end{aligned} \tag{20}$$

where

$$\begin{aligned}\Omega_c(t) \equiv&[\Delta_S(x_1) - \Delta_S(x_2)]/2\\ =&\frac{E^2d^2}{\omega-\nu_s}\sin(kr)\sin(\nu t-\phi),\end{aligned} \tag{21}$$

and

$$\begin{aligned}\delta_u(t) \equiv&[\Delta_S(x_1) + \Delta_S(x_2)]/2\\ =&\frac{E^2d^2}{\omega-\nu_s}[1+\cos(kr)\cos(\nu t-\phi)].\end{aligned} \tag{22}$$

For the sake of simplicity we set $\phi = 0$, which does not change any results in the EIT absorption.

APPENDIX C. EIT SPECTRA OF SUPERRADIANT AND SUBRADIANT STATES WITHOUT RWA OF THE COUPLING FIELD

In this section, we calculate the EIT absorption spectra of two atoms dressed by a moving standing wave. The total Hamiltonian can be written as

$$H' = H_0 + H_I, \tag{23}$$

where

$$H_0 = [\omega_+ + \delta_u(t)]|+\rangle\langle+| + [\omega_- + \delta_u(t)]|-\rangle\langle-|, \tag{24}$$

and

$$\begin{aligned}H_I =&\Omega_c(t)(|+\rangle\langle-| + |-\rangle\langle+|)\\ &-\Omega_p\left(e^{-i\nu_p t}|+\rangle\langle gg| + h.c.\right).\end{aligned} \tag{25}$$

We transform the wave function into the interaction picture,

$$|\psi_I\rangle = U_0(t)|\psi_S\rangle, \tag{26}$$

where $U_0(t) = \exp\left[\frac{i}{\hbar}\int_0^t dt' H_0(t')\right]$. The Schrödinger equation in the interaction picture is $i\hbar\partial_t|\psi_I\rangle = V|\psi_I\rangle$ with the interaction Hamiltonian

$$\begin{aligned}V =&U_0(t)H_I U_0^{-1}(t)\\ =&-\left[\left(\Omega_r + \Omega_{cr}e^{i2\nu t}\right)e^{i\delta_c t}|+\rangle\langle-| + h.c.\right]\\ &-\left[\Omega_p e^{i\delta_p t + if\sin\nu t}|+\rangle\langle gg| + h.c.\right],\end{aligned} \tag{27}$$

where the detuning of the probe field $\delta_p = \omega_+ + \Omega_0 - \nu_p$, the detuning of the driving field $\delta_c = 2\Delta_c - \nu$, the coupling strength of rotating terms $\Omega_r = -i\Omega_0\sin(kr)/2$, the coupling strength of counter rotating terms $\Omega_{cr} = i\Omega_0\sin(kr)/2$ and $f = \Omega_0\cos(kr)/\nu$.

We rewrite the master equation in Eq. (9) in the basis of the $|\pm\rangle$ states,

$$\begin{aligned}\frac{\partial\rho}{\partial t} =&-i[V,\rho] + \sum_{j=+,-}\frac{\gamma_j}{2}[2|gg\rangle\langle j|\rho|j\rangle\langle gg|\\ &-|j\rangle\langle j|\rho - \rho|j\rangle\langle j|].\end{aligned} \tag{28}$$

The dynamic evolution of the relevant matrix elements are

$$\frac{\partial \rho_{+gg}}{\partial t} = i\Omega_p e^{i\delta_p t + if\sin\nu t}\left(\rho_{gggg} - \rho_{++}\right) + i\left(\Omega_r + \Omega_{cr}e^{i2\nu t}\right)e^{i\delta_c t}\rho_{-gg} - \frac{\gamma_+}{2}\rho_{+gg}, \quad (29)$$

and

$$\frac{\partial \rho_{-gg}}{\partial t} = -i\Omega_p e^{i\delta_p t + if\sin\nu t}\rho_{-+} + i\left(\Omega_r^* + \Omega_{cr}^* e^{-i2\nu t}\right)e^{-i\delta_c t}\rho_{+gg} - \frac{\gamma_-}{2}\rho_{-gg}, \quad (30)$$

where $\rho_{gggg} = \langle gg|\rho|gg\rangle$, $\rho_{\pm gg} = \langle \pm|\rho|gg\rangle$ and $\rho_{+-} = \langle +|\rho|-\rangle$. For a weak probe field, the population is mainly in the level $|gg\rangle$. To the first order of Ω_p, we make the approximation $\rho_{gggg} = 1$, $\rho_{++} = \rho_{--} = \rho_{-+} = 0$. By introducing

$$\rho_{+gg} = e^{i\delta_p t}\tilde{\rho}_{+gg}, \quad (31)$$

and

$$\rho_{-gg} = e^{i(\delta_p - \delta_c)t}\tilde{\rho}_{-gg}, \quad (32)$$

we obtain the dynamic evolution of the slowly varying components,

$$\frac{\partial \tilde{\rho}_{+gg}}{\partial t} = \left(-i\delta_p - \frac{\gamma_+}{2}\right)\tilde{\rho}_{+gg} + i\left(\Omega_r + \Omega_{cr}e^{i2\nu t}\right)\tilde{\rho}_{-gg} + i\Omega_p e^{if\sin\nu t}, \quad (33)$$

$$\frac{\partial \tilde{\rho}_{-gg}}{\partial t} = \left(-i\delta_{2ph} - \frac{\gamma_-}{2}\right)\tilde{\rho}_{-gg} + i\left(\Omega_r^* + \Omega_{cr}^* e^{-i2\nu t}\right)\tilde{\rho}_{+gg}, \quad (34)$$

where $\delta_{2ph} = \delta_p - \delta_c$. According to the Floquet theory, the steady-state solution of equations (33) and (34) can be expanded in a Fourier series,

$$\tilde{\rho}_{+gg} = \sum_n \tilde{\rho}_{+gg}^{[n]} e^{in\nu t}, \quad (35)$$

$$\tilde{\rho}_{-gg} = \sum_n \tilde{\rho}_{-gg}^{[n]} e^{in\nu t}. \quad (36)$$

Substituting Eq. (35) and Eq. (36) into Eq. (33) and Eq. (34), and using the following expansion

$$\exp\left(if\sin\nu t\right) = \sum_k J_k\left(f\right)e^{ik\nu t} \quad (37)$$

where $J_k(f)$ is the kth order Bessel function of the first kind, we obtain

$$\frac{\partial}{\partial t}\tilde{\rho}_{+gg}^{[n]} = \left(-i\delta_p - \frac{\gamma_+}{2} - in\nu\right)\tilde{\rho}_{+gg}^{[n]} + i\Omega_r\tilde{\rho}_{-gg}^{[n]} + i\Omega_{cr}\tilde{\rho}_{-gg}^{[n-2]} + i\Omega_p J_n\left(f\right), \quad (38)$$

$$\frac{\partial}{\partial t}\tilde{\rho}_{-gg}^{[n]} = \left(-i\delta_{2ph} - \frac{\gamma_-}{2} - in\nu\right)\tilde{\rho}_{-gg}^{[n]} + i\Omega_r^*\tilde{\rho}_{+gg}^{[n]} + i\Omega_{cr}^*\tilde{\rho}_{+gg}^{[n+2]}. \quad (39)$$

In the steady state, $\partial\rho_{+gg}^{[n]}/\partial t = 0$ and $\partial\rho_{-gg}^{[n]}/\partial t = 0$, we obtain

$$\left(\delta_p - i\frac{\gamma_+}{2} + n\nu\right)\tilde{\rho}_{+gg}^{[n]} = \Omega_r\tilde{\rho}_{-gg}^{[n]} + \Omega_{cr}\tilde{\rho}_{-gg}^{[n-2]} + \Omega_p J_n\left(f\right), \quad (40)$$

$$\left(\delta_{2ph} - i\frac{\gamma_-}{2} + n\nu\right)\tilde{\rho}_{-gg}^{[n]} = \Omega_r^*\tilde{\rho}_{+gg}^{[n]} + \Omega_{cr}^*\tilde{\rho}_{+gg}^{[n+2]}. \quad (41)$$

From Eq. (41), we obtain

$$\tilde{\rho}_{-gg}^{[n]} = \frac{\Omega_r^*\tilde{\rho}_{+gg}^{[n]} + \Omega_{cr}^*\tilde{\rho}_{+gg}^{[n+2]}}{\delta_{2ph} - i\gamma_-/2 + n\nu}. \quad (42)$$

Substituting Eq. (42) into Eq. (40), we obtain

$$\begin{aligned}\left(\delta_p - i\frac{\gamma_+}{2} + n\nu\right)\tilde{\rho}_{+gg}^{[n]} =& \Omega_r\frac{\Omega_r^*\tilde{\rho}_{+gg}^{[n]} + \Omega_{cr}^*\tilde{\rho}_{+gg}^{[n+2]}}{\delta_{2ph} + n\nu - i\gamma_-/2} + \Omega_{cr}\frac{\Omega_r^*\tilde{\rho}_{+gg}^{[n-2]} + \Omega_{cr}^*\tilde{\rho}_{+gg}^{[n]}}{\delta_{2ph} + (n-2)\nu - i\gamma_-/2} + \Omega_p J_n\left(f\right) \\ =& \left[\frac{|\Omega_r|^2}{\delta_{2ph} + n\nu - i\gamma_-/2} + \frac{|\Omega_{cr}|^2}{\delta_{2ph} + (n-2)\nu - i\gamma_-/2}\right]\tilde{\rho}_{+gg}^{[n]} \\ &+ \frac{\Omega_r\Omega_{cr}^*}{\delta_{2ph} + n\nu - i\gamma_-/2}\tilde{\rho}_{+gg}^{[n+2]} + \frac{\Omega_r^*\Omega_{cr}}{\delta_{2ph} + (n-2)\nu - i\gamma_-/2}\tilde{\rho}_{+gg}^{[n-2]} + \Omega_p J_n\left(f\right). \quad (43)\end{aligned}$$

By defining the following quantities

$$P_n = \left(\delta_p + n\nu - i\gamma_+/2\right) - \left(R_n|\Omega_r|^2 + R_{n-2}|\Omega_{cr}|^2\right), \quad (44)$$

and

$$R_n = \frac{1}{\delta_{2ph} + n\nu - i\gamma_-/2}, \quad (45)$$

Eq. (43) can be rewritten as

$$P_n\tilde{\rho}^{[n]}_{+gg} = R_n\Omega_r\Omega^*_{cr}\tilde{\rho}^{[n+2]}_{+gg} + R_{n-2}\Omega^*_r\Omega_{cr}\tilde{\rho}^{[n-2]}_{+gg} + \Omega_p J_n(f). \tag{46}$$

The above linear equations can be solved numerically.

After we obtain $\tilde{\rho}^{[n]}_{+gg}$, we need to transform it back to the Schrödinger picture

$$\begin{aligned}\rho_{+gg} &\to U_0^{-1}(t)\rho_{+gg}U_0(t)\\ &= e^{-i(\omega_+ + \Omega_0)t - if\sin\nu t}e^{i\delta_p t}\tilde{\rho}_{+gg}\\ &= e^{-if\sin\nu t}\tilde{\rho}_{+gg}e^{-i\nu_p t}.\end{aligned} \tag{47}$$

Therefore, the zero frequency coherence in the Schrödinger picture is

$$\rho^{[0]}_{+gg} = \sum_n J_{-n}(-f)\,\tilde{\rho}^{[n]}_{+gg}. \tag{48}$$

The absorption is proportional to $\mathrm{Im}\rho^{[0]}_{+gg}$.

APPENDIX D. DERIVATION OF THE CAVITY REFLECTION COEFFICIENT

In this section we follow the procedure in refs. [40, 44] to calculate the x-ray reflection coefficient R of the planar cavity as sketched in the main text Fig. 3,

$$R = \frac{\langle a_{out}\rangle}{a_{in}}, \tag{49}$$

where a_{in} and a_{out} are the field amplitudes of the incident and output x-ray fields. The output field operator can be calculated by using the input-output formalism [45],

$$\begin{aligned}a_{out} =& -a_{in}\left(\hat{\mathbf{a}}^*_{out}\cdot\hat{\mathbf{a}}_{in}\right)\\ &+\sqrt{2\kappa_R}\left[\left(\hat{\mathbf{a}}^*_{out}\cdot\hat{\mathbf{a}}_1\right)a_1 + \left(\hat{\mathbf{a}}^*_{out}\cdot\hat{\mathbf{a}}_2\right)a_2\right].\end{aligned} \tag{50}$$

where $\hat{\mathbf{a}}_1$ and $\hat{\mathbf{a}}_2 = \hat{\mathbf{a}}_1\times\hat{\mathbf{k}}$ are the unit polarization vectors of two cavity modes with annihilation operators a_1 and a_2, $\mathbf{k}$ is the wave vector of the incident x ray and κ_R characterizes the coupling between the output (and input) field and the cavity modes. The Hamiltonians of the cavity and the nucleus in the interaction picture are [40, 44]

$$\begin{aligned}H_C =& \Delta_{CA}a_1^\dagger a_1 + \Delta_{CA}a_2^\dagger a_2\\ &+\sum_{j=1}^{2} i\sqrt{2\kappa_R}\left[\left(\hat{\mathbf{a}}^*_j\cdot\hat{\mathbf{a}}_{in}\right)a_{in}a_j^\dagger - \left(\hat{\mathbf{a}}^*_{in}\cdot\hat{\mathbf{a}}_j\right)a^*_{in}a_j\right],\end{aligned} \tag{51}$$

$$\begin{aligned}H_N =& \sum_{n=1}^{N}\left[\frac{\delta_g}{2}|g_n\rangle\langle g_n| + \left(-\frac{\delta_e}{2}-\Delta\right)|e_n\rangle\langle e_n|\right]\\ &+\sum_{n=1}^{N}\left[-\frac{\delta_g}{2}|b_n\rangle\langle b_n| + \left(\frac{\delta_e}{2}-\Delta\right)|a_n\rangle\langle a_n|\right]\\ &+\sum_{j=1}^{2}\left[\left(\hat{\mathbf{d}}^*\cdot\hat{\mathbf{a}}_j\right)gS_+a_j + \left(\hat{\mathbf{d}}\cdot\hat{\mathbf{a}}^*_j\right)g^*a_j^\dagger S_-\right],\end{aligned} \tag{52}$$

where $\Delta_{CA} = \omega_C - \nu_p$ is the cavity detuning, $\Delta = \nu_p - \omega$ is the energy difference between the external x-ray field and the bare transition frequency of the nucleus, $S_+ = \sum_{n=1}^{N}(|e_n\rangle\langle g_n| + |a_n\rangle\langle b_n|)$ and $S_- = S_+^\dagger$ are the nuclear collective raising and lowering operators, g is the coupling strength between the cavity mode and the nuclei, and $\hat{\mathbf{d}}$ is the unit vector of the transition dipole moment. Since the magnetic field is parallel to the direction of the electric field of input x ray, there are only two linearly polarized transitions can happen between states ($|g\rangle$, $|e\rangle$) and ($|b\rangle$, $|a\rangle$), respectively. The Heisenberg equation for the operator a_j,

$$\frac{d}{dt}a_j = i\left[H_C + H_N, a_j\right] - \kappa a_j, \tag{53}$$

where κ is the decay rate of the cavity. In the bad cavity regime, which is the situation for the thin-film cavities, κ is large. In the steady state, $da_j/dt = 0$ and we have

$$a_j = \frac{\sqrt{2\kappa_R}\left(\hat{\mathbf{a}}^*_j\cdot\hat{\mathbf{a}}_{in}\right)a_{in} - i\left(\hat{\mathbf{d}}\cdot\hat{\mathbf{a}}^*_j\right)g^*S^-}{\kappa + i\Delta_{CA}}. \tag{54}$$

Inserting Eq. (54) into Eq. (50), we obtain the reflection coefficient

$$\begin{aligned}R =& \left(\frac{2\kappa_R}{\kappa+i\Delta_{CA}} - 1\right)\left(\hat{\mathbf{a}}^*_{out}\cdot\hat{\mathbf{a}}_{in}\right)\\ &- i\frac{1}{a_{in}}\frac{\sqrt{2\kappa_R}}{\kappa+i\Delta_{CA}}\left[\hat{\mathbf{d}}\cdot\left(\hat{\mathbf{a}}_1\hat{\mathbf{a}}^*_1 + \hat{\mathbf{a}}_2\hat{\mathbf{a}}^*_2\right)\cdot\hat{\mathbf{a}}^*_{out}\right]g^*\left\langle S^-\right\rangle\\ =& \left(\frac{2\kappa_R}{\kappa+i\Delta_{CA}} - 1\right)\left(\hat{\mathbf{a}}^*_{out}\cdot\hat{\mathbf{a}}_{in}\right)\\ &- i\frac{1}{a_{in}}\frac{\sqrt{2\kappa_R}}{\kappa+i\Delta_{CA}}\left(\hat{\mathbf{a}}^*_{out}\cdot\hat{\mathbf{a}}_{in}\right)\sqrt{2N}g^*\rho_{+G}.\end{aligned} \tag{55}$$

In the above equation, the first part is due to the direct reflection of the incident light a_{in} from the cavity. In Fig. 4 in the main text we use typical parameters [40] $\kappa = 45\xi$ and $\kappa_R = 25\xi$ with $\xi = 18000\gamma_0$ a scaling factor. The cooperative factor $\sqrt{2N}g^* = \sqrt{1400\xi}$. For the collective Lamb shift $\omega_0 = 10\gamma_0$, the cavity detuning should be $\Delta_{CA} = 34\xi$. Due to the cooperative effect, the second term in Eq. (55) is dominant, although in Fig. 4 we included both terms. The reflectance is approximately,

$$|R|^2 \propto |\rho_{+G}|^2, \tag{56}$$

where ρ_{+G} can be calculated following the same procedure as in the section III. Typically, $\rho_{+G}(t) =$

$\sum_n \rho_{+G}^{[n]} e^{i2\nu t}$ has multiple frequency components. The reflectance is an average over time and in the time scale $T \gg 1/\nu$,

$$|R|^2 \propto \lim_{T\to\infty} \frac{1}{T} \int_0^T |\rho_{+G}(t)|^2 \mathrm{d}t = \sum_n \left|\rho_{+G}^{[n]}\right|^2 . \qquad (57)$$

Only when $\nu = 0$, we come back to the case of static coupling field as described in [40]. There is only a single frequency in ρ_{+G} and no time average is needed.

[1] K.-J. Boller, A. Imamoğlu, and S. E. Harris, Phys. Rev. Lett. **66**, 2593 (1991).
[2] M. Fleischhauer, A. Imamoğlu, and J. P. Marangos, Rev. Mod. Phys. **77**, 633 (2005).
[3] L. V. Hau, S. E. Harris, Z. Dutton, and C. H. Behroozi, Nature (London) **397**, 594 (1999).
[4] M. M. Kash, V. A. Sautenkov, A. S. Zibrov, L. Hollberg, G. R. Welch, M. D. Lukin, Y. Rostovtsev, E. S. Fry, and M. O. Scully, Phys. Rev. Lett. **82**, 5229 (1999).
[5] O. Kocharovskaya, Y. Rostovtsev, and M. O. Scully, Phys. Rev. Lett. **86**, 628 (2001).
[6] M. Fleischhauer and M. D. Lukin, Phys. Rev. Lett. **84**, 5094 (2000).
[7] M. Fleischhauer and M. D. Lukin, Phys. Rev. A **65**, 022314 (2002).
[8] M. D. Lukin, Rev. Mod. Phys. **75**, 457 (2003).
[9] S. E. Harris, J. E. Field, and A. Imamoglu, Phys. Rev. Lett. **64**, 1107 (1990).
[10] M. Jain, H. Xia, G. Y. Yin, A. J. Merriam, and S. E. Harris, Phys. Rev. Lett. **77**, 4326 (1996).
[11] R. Röhlsberger, K. Schlage, B. Sahoo, S. Couet, and R. Rüffer, Science **328**, 1248 (2010).
[12] P. Anisimov, Y. Rostovtsev, and O. Kocharovskaya, Phys. Rev. B **76**, 094422 (2007).
[13] I. Tittonen, M. Lippmaa, E. Ikonen, J. Lindén, and T. Katila, Phys. Rev. Lett. **69**, 2815 (1992).
[14] Mark Bates, Timothy R. Blosser, and Xiaowei Zhuang, Phys. Rev. Lett. **94**, 108101 (2005).
[15] R. Röhlsberger, H.-C. Wille, K. Schlage, and B. Sahoo, Nature (London) **482**, 199 (2012).
[16] D. Z. Xu, Yong Li, C. P. Sun, and Peng Zhang, Phys. Rev. A **88**, 013823 (2013).
[17] A. A. Makarov, Phys. Rev. A **92**, 053840 (2015).
[18] R. H. Dicke, Phys. Rev. **93**, 99 (1954).
[19] R. H. Lehmberg, Phys. Rev. A **2**, 883 (1970); **2**, 889 (1970).
[20] G. S. Agarwal, in *Quantum Statistical Theories of Spontaneous Emission and Their Relation to Other Approaches*, edited by G. Höhler, Springer Tracts in Modern Physics Vol. 70 (Springer, Berlin, 1974).
[21] M. O. Scully, Phys. Rev. Lett. **102**, 143601 (2009).
[22] M. Scully, Laser Phys. **17**, 635 (2007) .
[23] D. W. Wang, Z. H. Li, H. Zheng, and S.-Y. Zhu, Phys. Rev. A **81**, 043819 (2010).
[24] D. Petrosyan and G. Kurizki, Phys. Rev. Lett. **89**, 207902 (2002).
[25] A. Muthukrishnan, G. S. Agarwal, and M. O. Scully, Phys. Rev. Lett. **93**, 093002 (2004).
[26] P. Grangier, A. Aspect, and J. Vigue, Phys. Rev. Lett. **54**, 418 (1985).
[27] R. G. DeVoe and R. G. Brewer, Phys. Rev. Lett. **76**, 2049 (1996).
[28] C. Hettich, C. Schmitt, J. Zitzmann, S. Kühn, I. Gerhardt, and V. Sandoghdar, Science **298**, 385 (2002).
[29] A. Gaetan, Y. Miroshnychenko, T. Wilk, A. Chotia, M. Viteau, D. Comparat, P. Pillet, A. Browaeys, and P. Grangier, Nature Physics, **5** (2), 115 (2009).
[30] B. H. McGuyer, M. McDonald, G. Z. Iwata, M. G. Tarallo, W. Skomorowski, R. Moszynski, and T. Zelevinsky, Nature Physics **11**, 32 (2016).
[31] G. V. Varada and G. S. Agarwal, Phys. Rev. A **45**, 6721 (1992).
[32] G. S. Agarwal and N. Nayak, J. Opt. Soc. Am. B **1**, 164 (1984).
[33] D.-W. Wang, R.-B. Liu, S.-Y. Zhu, and M. O. Scully, Phys. Rev. Lett. **114**, 043602 (2015).
[34] J.-T. Chang, J. Evers, M. O. Scully, and M. S. Zubairy, Phys. Rev. A **73**, 031803 (2006).
[35] D.-W. Wang and M. O. Scully, Phys. Rev. Lett. **113**, 083601 (2014)
[36] M. Mücke, E. Figueroa, J. Bochmann, C. Hahn, K. Murr, S. Ritter, C. J. Villas-Boas, and G. Rempe, Nature **465**, 755 (2010).
[37] S. Trotzky, Y.-A. Chen, U. Schnorrberger, P. Cheinet, and I. Bloch, Phys. Rev. Lett. **105**, 265303 (2010).
[38] A. Sipahigil1, R. E. Evans1, D. D. Sukachev, M. J. Burek, J. Borregaard, M. K. Bhaskar, C. T. Nguyen, J. L. Pacheco, H. A. Atikian, C. Meuwly, R. M. Camacho, F. Jelezko, E. Bielejec, H. Park1, M. Loncar, and M. D. Lukin, Science **354**, 847 (2016).
[39] M. O. Scully, E. S. Fry, C. H. R. Ooi, and K.Wodkiewicz, Phys. Rev. Lett. **96**, 010501 (2006).
[40] K. P. Heeg and J. Evers, Phys. Rev. A **88**, 043828 (2013).
[41] M. O. Scully, Phys. Rev. Lett. **115**, 243602 (2015).
[42] K. P. Heeg, H.-C. Wille, K. Schlage, T. Guryeva, D. Schumacher, I. Uschmann, K. S. Schulze, B. Marx, T. Kämpfer, G. G. Paulus, R. Röhlsberger, and J. Evers, Phys. Rev. Lett. **111**, 073601 (2013).
[43] J. Hannon and G. Trammell, Hyperfine Interact. **123-124**, 127 (1999).
[44] K. P. Heeg and J. Evers, Phys. Rev. A **91**, 063803 (2015).
[45] C. Gardiner and P. Zoller, *Quantum Noise: A. Handbook of Markovian and Non-Markovian Quantum Stochastic Methods with Applications to Quantum Optics*, Springer Series in Synergetics (Springer, Heidelberg, 2004).